MOLECULAR AND CELLULAR BIOLOGY, Oct. 2006, p. 7791–7805 Vol. 26, No. 20
0270-7306/06/$08.00+0 doi:10.1128/MCB.00022-06

Different Routes of Bone Morphogenic Protein (BMP) Receptor Endocytosis Influence BMP Signaling▽†

Anke Hartung,[1]‡ Keren Bitton-Worms,[2]‡ Maya Mouler Rechtman,[2] Valeska Wenzel,[1] Jan H. Boergermann,[3] Sylke Hassel,[3] Yoav I. Henis,[2] and Petra Knaus[1,3]*

Department of Physiological Chemistry II, University of Wuerzburg, Wuerzburg, Germany[1]; Department of Neurobiochemistry, George S. Wise Faculty of Life Science, Tel Aviv University, Tel Aviv, Israel[2]; and Institute for Biochemistry, FU Berlin, Berlin, Germany[3]

Received 5 January 2006/Returned for modification 6 March 2006/Accepted 31 July 2006

Endocytosis is important for a variety of functions in eukaryotic cells, including the regulation of signaling cascades via transmembrane receptors. The internalization of bone morphogenetic protein (BMP) receptor type I (BRI) and type II (BRII) and its relation to signaling were largely unexplored. Here, we demonstrate that both receptor types undergo constitutive endocytosis via clathrin-coated pits (CCPs) but that only BRII undergoes also caveola-like internalization. Using several complementary approaches, we could show that (i) BMP-2-mediated Smad1/5 phosphorylation occurs at the plasma membrane in nonraft regions, (ii) continuation of Smad signaling resulting in a transcriptional response requires endocytosis via the clathrin-mediated route, and (iii) BMP signaling leading to alkaline phosphatase induction initiates from receptors that fractionate into cholesterol-enriched, detergent-resistant membranes. Furthermore, we show that BRII interacts with Eps15R, a constitutive component of CCPs, and with caveolin-1, the marker protein of caveolae. Taken together, the localization of BMP receptors in distinct membrane domains is prerequisite to their taking different endocytosis routes with specific impacts on Smad-dependent and Smad-independent signaling cascades.

The endocytosis of transmembrane receptors by clathrin-dependent and -independent pathways plays a major role in the control of receptor density at the cell surface (21). The most common and best-characterized endocytic route is via clathrin-coated pits (CCPs). Internalized cell surface receptors undergo either recycling to the plasma membrane or transport to lysosomes for degradation (32). Furthermore, CCP-mediated endocytosis was proposed to be required for the signaling of several transmembrane receptors (7, 11, 42).

Cholesterol-enriched domains were demonstrated in artificial lipid bilayers and proposed to exist in cell membranes as lipid rafts (5, 63, 64). Insolubility in cold nonionic detergents, resulting in detergent-resistant membrane fractions (DRMs), became the biochemical fingerprint of raft-resident proteins, although this is clearly an operational definition that depends on the detergent and extraction conditions (30, 64). The raft hypothesis has gained widespread but not general acceptance, and there is considerable debate about the existence and characteristics of rafts in biological membranes (2, 12, 43, 61). An alternative hypothesis is that cholesterol plays a role in the formation of lipid shells, small dynamic lipid-cholesterol assemblies that can associate with proteins; accordingly, specific protein interactions are involved in forming the larger cholesterol-dependent structures in the membrane (2). Lipid rafts were proposed to function in membrane protein sorting and in the formation of signaling complexes, as well as in endocytic trafficking (60, 64).

Caveolae are membrane invaginations containing the integral membrane protein caveolin (36, 55) and are considered to be a subset of lipid rafts. They display the detergent insolubility features of DRMs, but DRMs are also highly abundant in cells lacking caveolae and caveolin-1 (cav-1). Caveolae were reported to be involved in potocytosis (3), endocytosis, and the regulation of signaling cascades (1, 47). While some publications describe caveolae as stable, immobile structures not involved in endocytic trafficking (68), others have revealed cav-1-positive, EEA-1-negative, and transferrin-negative vesicles (caveosomes) using real-time video microscopy (48, 49).

Bone morphogenetic proteins (BMPs) are members of the transforming growth factor β (TGF-β) superfamily and are involved in the regulation of proliferation, differentiation, chemotaxis, and apoptosis (28, 40). BMP signaling involves two types of transmembrane serine/threonine kinases, BMP type I and type II receptors (BRI and BRII, respectively) (6, 29). BMP receptor activation occurs upon ligand binding to preformed receptor complexes (PFCs) or BMP-induced signaling complexes (BISCs) composed of BRI and BRII. Binding of BMP-2 to PFCs results in activation of the Smad pathway, whereas BISCs initiate the activation of Smad-independent, p38-dependent pathways, resulting in the induction of alkaline phosphatase (ALP) (45).

BMP receptor endocytosis has not been extensively studied, and the potential role of localization to different regions of the plasma membrane in determining the signaling pathways activated by PFCs and BISCs has not been explored. One report that suggests such involvement showed that cav-1 isoforms

* Corresponding author. Mailing address: Institute for Chemistry/Biochemistry, FU Berlin, Thielallee 63, 14195 Berlin, Germany. Phone: 49 (0)30-838 52935. Fax: 49 (0)30-838 51935. E-mail: knaus@chemie.fu-berlin.de.

† Supplemental material for this article may be found at http://mcb.asm.org/.

‡ These authors contributed equally to the manuscript.

▽ Published ahead of print on 21 August 2006.

bind to overexpressed BRII and that cav-1α influences Smad signaling in A431 cells (46).

Beyond that, the present work shows that BRI and BRII are continuously internalized via clathrin-mediated endocytosis; additionally, BRII is endocytosed via a caveola- and cholesterol-dependent route. BMP-2 binding to PFCs induces Smad1/5 phosphorylation at the plasma membrane, while continuation of Smad signaling requires receptor endocytosis into CCPs. A second population of BMP receptors resides in DRMs, which is a prerequisite for Smad-independent signaling. Cholesterol depletion inhibits specifically BMP-2-mediated ALP production, while Smad signaling is unaffected. Inhibition of clathrin-mediated endocytosis affects also the induction of ALP, suggesting that both Smad-dependent and Smad-independent signaling pathways are required for BMP-2 induced ALP production. Our data demonstrate a distinct membrane localization of BMP receptors for specific signaling properties and a tight regulation of signaling by different endocytic routes.

MATERIALS AND METHODS

Materials. The cell lines C2C12, 293T, and COS7 were from the American Type Culture Collection, mouse monoclonal immunoglobulin G (IgG) against the hemagglutinin (HA) tag (12CA5) was from Roche, antibody against cav-1α and small interfering RNA (siRNA) specific for cav-1 were from Santa Cruz Biotechnology, phospho-Smad1/5-specific antibody was from Cell Signaling, peroxidase-coupled goat anti-mouse IgG and goat anti-rabbit IgG were from Dianova, and Alexa 546-goat anti-mouse $F(ab')_2$ was from Molecular Probes. Fluorescent $F(ab')_2$ was converted to Fab′ as described by us earlier (18). Goat IgG was from Jackson ImmunoResearch Laboratories, and anti-myc (9E10) antibody (14) was from Harvard Monoclonal Antibodies. Lovastatin was from CALBIOCHEM, Lipofectamine was from Invitrogen, polyethylenimine was from Aldrich, and DEAE-dextran was from Amersham Biosciences. Plasmids encoding the HA-tagged wild-type (wt) dynamin 2 (dyn2) protein and dyn2 with the K44A mutation (dyn2-K44A) were a gift of S. Schmid (The Scripps Research Institute, La Jolla, CA).

Separation of detergent-insoluble membrane domains. Stably transfected C2C12 cells (45) or transiently transfected 293T cells were lysed with TNE-CHAPS buffer (20 mM CHAPS {3-[(3-cholamidopropyl)-dimethylammonio]-1-propanesulfonate}, 25 mM Tris-HCl [pH 7.4], 150 mM NaCl, 3 mM EDTA, protease inhibitor cocktail [Roche], 1 mM phenylmethylsulfonyl fluoride [PMSF]) and homogenized using a Potter apparatus (five strokes at 1,000 rpm, 4°C). An OptiPrep (Axis-Shield) concentration of 40% was adjusted in the lysate, and a discontinuous OptiPrep gradient (30%, 5%) was formed above the lysate. After ultracentrifugation (39,000 rpm, 20 h, 4°C; SW40Ti Beckman rotor), the gradient was fractionated at 4°C from the top by pipetting 12 1-ml fractions. Fractions were analyzed using sodium dodecyl sulfate-polyacrylamide gel electrophoresis (SDS-PAGE) and Western blotting.

Coimmunoprecipitation. Stably transfected C2C12 cells (45) were lysed in TNE lysis buffer (25 mM Tris-HCl [pH 7.5], 150 mM NaCl, 5 mM EDTA, 1% Triton X-100, 60 mM *n*-octyl-D-glucoside, proteinase inhibitor cocktail [Roche], 1 mM PMSF). Immunoprecipitation was accomplished using 1 μg cav-1α antibody. For investigation of ligand effect, cells were starved in Dulbecco's modified Eagle's medium (DMEM) plus 0.5% fetal calf serum (FCS) for 2 h, followed by stimulation with 20 nM BMP-2 for 30 min.

Immunofluorescence microscopy. COS7 or C2C12 cells were grown on glass coverslips. Incubations for various treatments to inhibit endocytosis were timed such that the labeling with fluorescent antibodies would start 48 h posttransfection. Prior to antibody labeling, cells were incubated (30 min, 37°C) with DMEM to allow digestion of serum-derived ligands. After being washed with cold Hanks' balanced salt solution (HBSS)-HEPES-bovine serum albumin (HBSS, 20 mM HEPES [pH 7.2], 2% bovine serum albumin), cells were incubated (4°C, 30 min) in the same buffer supplemented with normal goat IgG (200 μg/ml) to block nonspecific binding. This was followed by successive incubation (4°C, with three washes between incubations) with anti-myc or anti-HA mouse IgG (20 μg/ml, 45 min) and then Alexa 546–goat anti-mouse Fab′ (40 μg/ml, 30 min) in the same buffer. After being washed, labeled cells were either kept at 4°C (control) or incubated at 37°C for different periods. The cells were then fixed by successive incubation in methanol (5 min, −20°C) and acetone (2 min, −20°C) and mounted with ProLong antifade (Molecular Probes). Digital fluorescence images were acquired with a Leica DMRB/E microscope with a 100× oil immersion objective, coupled to a Magnafire charge-coupled-device camera (Optronics). Images were exported to and processed with Adobe Photoshop.

Electron microscopy. Preembedding immunogold labeling of HA-tagged BRII was accomplished on C2C12 cells on glass coverslips. The immunolabeling was carried out by applying anti-HA antibody for 1 h at 4°C, and after mild fixation with 4% paraformaldehyde for 10 min at 4°C, secondary antibody coupled to 12-nm colloidal gold beads was incubated for 2 h at room temperature. The cells were fixed with 2.5% glutaraldehyde and subsequently with 2% osmium tetroxide buffered in 0.05 M cacodylate buffer and after that contrasted using 0.5% uranyl acetate at 4°C overnight. Cells were dehydrated, embedded in EPON (Sigma), and, after polymerization at 60°C (for at least 24 h), ultrathin sectioned. Sections were analyzed with a Zeiss EM10 electron microscope (Zeiss) and processed with Adobe Photoshop.

As an alternative method, cells were centrifuged and the cell pellet was fixed using 4% paraformaldehyde. After dehydration, cells were embedded using LR-White (Science Services GmbH) in gelatin capsules. After polymerization at 40°C (for at least 3 days), ultrathin sections were incubated in primary-antibody solution (anti-HA and anti-cav-1α) and subsequently with gold-conjugated secondary reagents (6 nm goat anti-rabbit and 12 nm goat anti-mouse). Sections were fixed using glutaraldehyde and contrasted with uranyl acetate and Reynolds lead citrate.

Internalization measurements. Internalization of epitope-tagged BMP receptors was quantified by the point confocal method as described previously (13). The intensity measurement was performed using a fluorescence recovery after photobleaching setup described by us earlier (25) under nonbleaching illumination conditions. For that, cells were transfected with HA-BRIb or myc-BRII. The cell surface receptors were labeled at 4°C with anti-myc or anti-HA followed by Alexa 546–goat anti-mouse Fab′, as described for immunofluorescence microscopy. The cells were fixed (either immediately or following appropriate incubation at 37°C) and taken for the point confocal measurements.

Treatments affecting internalization and BMP signaling steps. Treatments employed to inhibit CCP-mediated endocytosis include hypertonic treatment, cytosol acidification, and incubation with chlorpromazine (CP). Hypertonic treatment (22, 27) and cytosol acidification (22, 27, 57) were performed as described previously (13). CP treatment (70, 72) was used in two alternative protocols: incubation with 100 μM CP in HBSS-HEPES buffer for 15 min at 37°C or incubation with 5 μM in growth medium for 16 to 72 h for BMP-2 signaling assays.

To inhibit caveola-like endocytosis, genistein, nystatin, or metabolic inhibition with lovastatin was employed. Cells were treated with genistein (4, 38) as described previously (53) by incubation with 200 μM genistein in MEM (60 min, 37°C). Treatment with nystatin (3) was employed by applying 25 μg/ml nystatin (in MEM containing 10 mM HEPES [pH 7.2]) for 30 min at 37°C. Cholesterol depletion using lovastatin was carried out as described previously (31, 37) by incubating C2C12 cells with 50 μM lovastatin and 50 μM mevalonate in DMEM plus 0.5% lipoprotein-deficient serum (LPDS) (prepared as described in reference 20). Incubation was for 16 to 72 h, depending on the type of the experiment and the required length of stimulation with BMP-2.

Analyzing BMP signaling. To detect Smad1/5 phosphorylation, cells were starved for 24 h, stimulated with 20 nM BMP-2 for 30 min, and lysed with TNE lysis buffer. Thirty micrograms of protein per lane was subjected to SDS-PAGE and Western blotting. For analyzing BMP-2-dependent transcriptional response, C2C12 cells were transfected with a BMP response element (BRE) luciferase reporter construct [$p(BRE)_4$-luc] (35), renilla luciferase (pRLTK) (Promega), and the DNA constructs indicated in Results. Cells were starved for 5 h and stimulated for 16 to 24 h with 1 nM BMP-2. Cell lysis and luciferase measurements were carried out according to the manufacturer's instructions (dual-luciferase assay system; Promega). For quantitative analysis of ALP activity, C2C12 cells were starved for 5 h and stimulated with 5, 50, or 100 nM BMP-2 for 72 h. ALP activity was determined as described by us earlier (45). For ALP measurements following cholesterol depletion by lovastatin treatment, C2C12 cells were incubated for 24 h in 10% LPDS (plus lovastatin and mevalonate [LM]) prior to starvation in 0.2% LPDS (plus LM). For real-time PCR measurements, RNA was isolated from C2C12 cells treated with or without lovastatin (as in ALP activity measurements) using peqGOLD TriFast (Peqlab) and reversed transcribed by Moloney murine leukemia virus reverse transcriptase (Promega). Real-time PCR was performed with the *Taq* CORE Kit10 (Q-BIOgene) using the Opticon 1 DNA engine (MJ Research). Primer sequences are available upon request.

RESULTS

BMP receptors float with DRM domains. cav-1 is a structural component of caveolae (36, 55), membrane invaginations enriched in cholesterol and sphingolipids proposed to comprise a specialized subpopulation of lipid rafts (2, 64). Proteins interacting with such regions are often identified by their insolubility in nonionic detergents, floating to a low density on sucrose or OptiPrep gradients after ultracentrifugation (5, 58). To verify whether BMP receptors reside in such domains, we separated DRMs from C2C12 or 293T cells by OptiPrep gradient ultracentrifugation.

The occurrence of BRIa in DRMs was investigated by coexpressing HA-tagged BRIa and cav-1α in 293T cells, which express very low endogenous levels of cav-1 (see Fig. SA1 in the supplemental material). Western blot analyses using anti-cav-1α antibodies identified fraction 6 (Fig. 1A, B, and D) or fraction 7 (Fig. 1C) as the main cav-1 fraction. The higher fractions resemble insoluble regions of the plasma membrane (i.e., lanes 10 to 12). BRIa was predominantly found in DRM fractions (Fig. 1A). To estimate the percentage of the receptor found in a special fraction, the density of each lane was measured and divided by the sum of the densities of all lanes. This analysis showed that 34% of BRIa is found in DRM fraction 6.

The distribution of BRIb was examined using C2C12 cells stably expressing HA-tagged BRIb. Thirty-five percent of BRIb floated to the main cav-1 fraction 6 (Fig. 1B).

BRII exists in two splice variants, the "long form" BRII (BRII-LF) and the "short-form" BRII (BRII-SF) (54). The distribution of these variants in the OptiPrep gradient was studied in C2C12 cells stably expressing HA-tagged BRII-LF or BRII-SF. Both BRII splice variants appear widely distributed over the gradient (Fig. 1C and see Fig. SA2 in the supplemental material). Twelve percent of total BRII-LF was found in the main cav-1-positive fraction, fraction 7 (Fig. 1C).

To exclude the possibility of cell type-specific differences in receptor distributions, we also examined 293T cells, transiently transfected with HA-tagged BRII-LF and cav-1α (compare levels of BRIa in Fig. 1A). In these cells, about 17% of BRII-LF cofractionated with overexpressed cav-1α in fraction 6 (Fig. 1D), suggesting that in both C2C12 and transfected 293T cells, similar percentages of the receptors cofractionate with cav-1α (compare the BRII-LF distributions in C2C12 cells in Fig. 1C). The addition of BMP-2 showed no alterations in both BRII and BRI distributions (data not shown). As an additional control, the same blots were examined for endogenous interleukin 2 receptor β (IL-2Rβ), reported to be concentrated in DRMs before stimulation with IL-2 (19). Indeed IL-2Rβ was found mainly in fraction 6, along with cav-1α (Fig. 1D, bottom panel).

In order to test whether BMP receptors can associate with DRMs in the absence of cav-1, we transfected cav-1-deficient 293T cells with receptor constructs but not with cav-1α. The results (Fig. 1A and D, bottom panels) demonstrate a significant association of BRIa and BRII-LF with DRM fractions, suggesting that both receptor types are present also in noncaveolar raft-like regions.

BMP receptors interact with cav-1α. To investigate whether the DRM-associated subpopulation of BRII and BRI interacts with cav-1, we performed coimmunoprecipitation experiments.

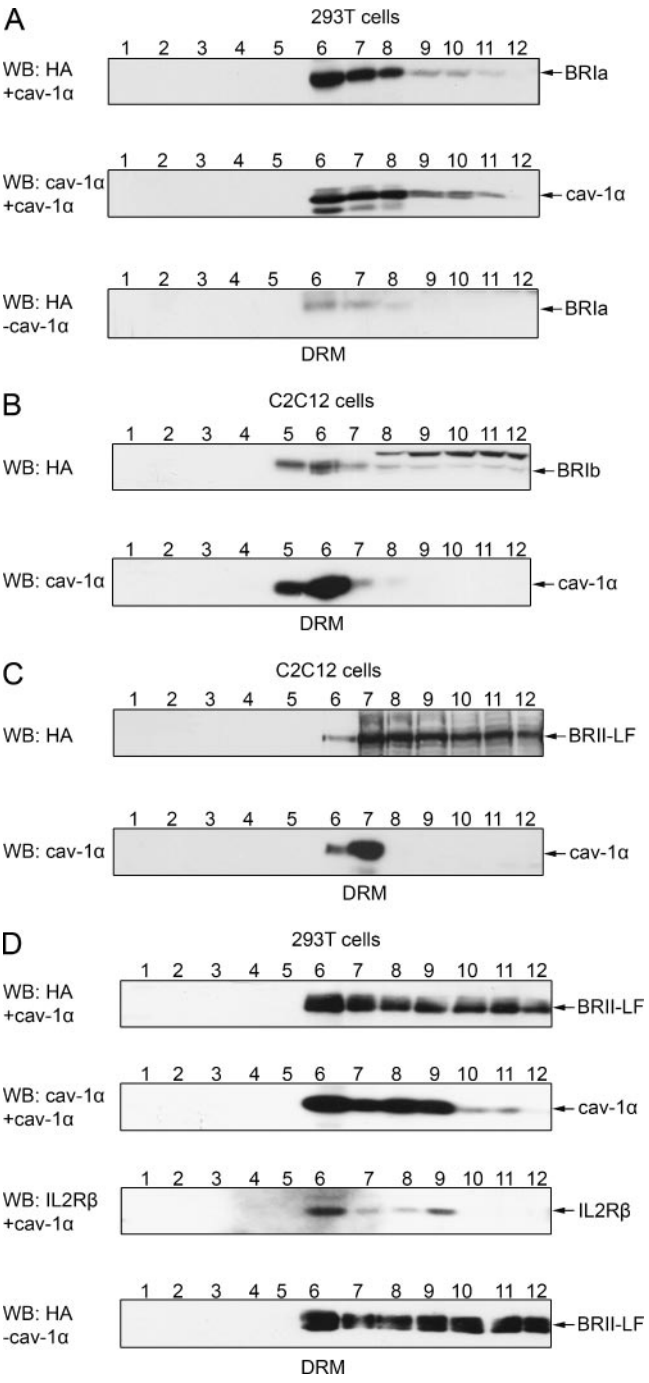

FIG. 1. BMP receptors float with DRM domains. BRIa, BRIb, and BRII distribution was studied in 293T (A and D) and C2C12 (B and C) cells. CHAPS lysates were subjected to Optiprep gradient fractionation and analyzed by Western blotting with anti-cav-1 or anti-HA antibodies. (A) BRIa, analyzed in 293T cells transfected with HA-BRIa and HA-cav-1α, is detected in DRM fractions. The distribution of BRIa was not altered when cav-1α was not transfected (bottom panel). (B) In C2C12 cells stably expressing HA-BRIb, the receptor cofractionates with endogenous cav-1α in DRM fractions. (C) C2C12 cells stably expressing HA-BRII-LF or (D) 293T cells transiently transfected with HA-BRII-LF and HA-cav-1α show a wide receptor distribution. Western blotting with IL-2Rβ-specific antibody verifies fraction 6 as the main DRM fraction. The distribution of BRII was not altered when no cav-1α was transfected (bottom panel). WB, Western blotting.

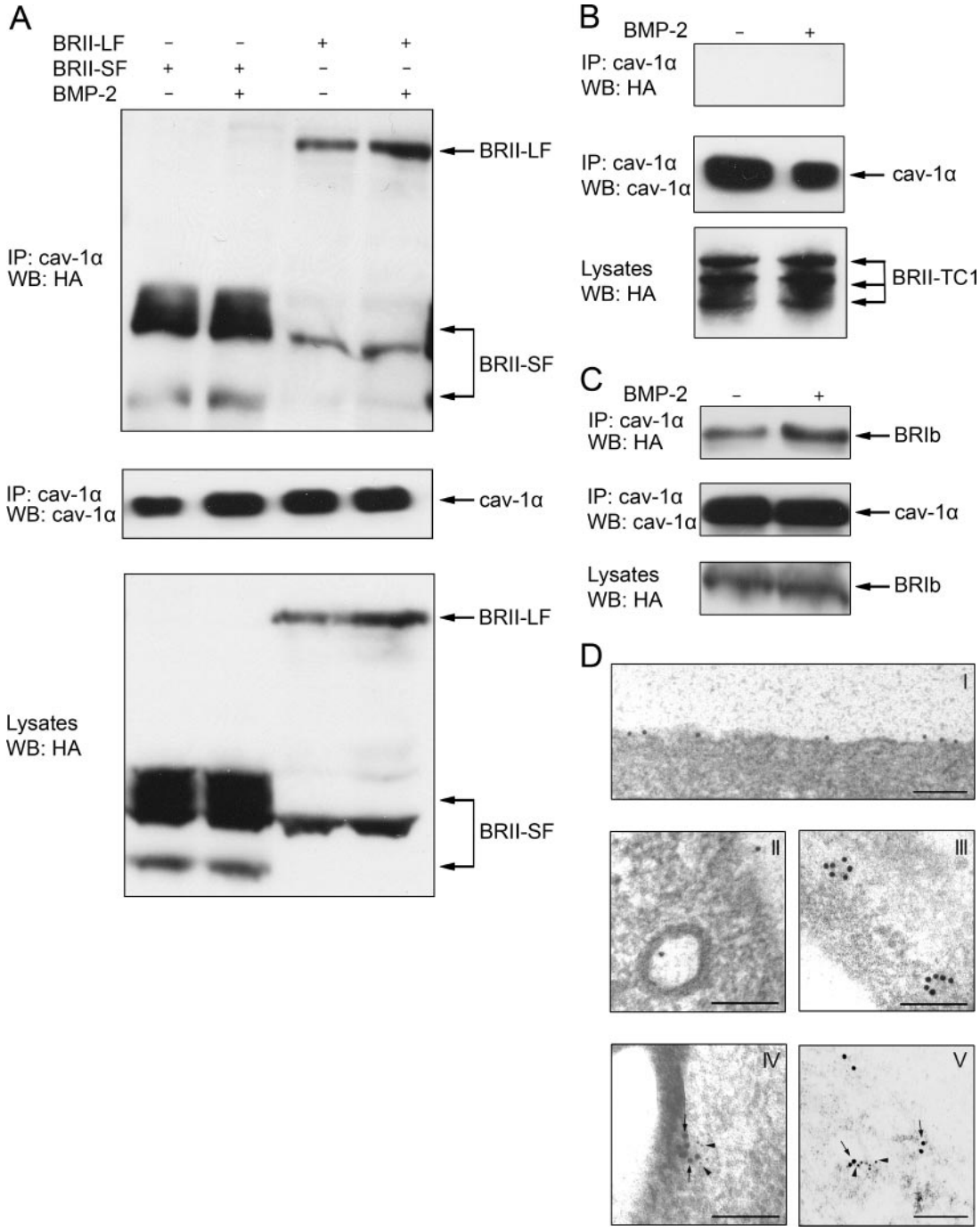

FIG. 2. BMP receptors interact and colocalize with endogenous cav-1α. cav-1α was immunoprecipitated from C2C12 cells stably expressing HA-tagged BRII-LF, BRII-SF, BRII-TC1, or BRIb (A to C). (A) BRII-LF and BRII-SF interact with cav-1α. BMP-2 stimulation shows no effect. (B) BRII-TC1 is not associated with cav-1α. (C) BRIb interacts with cav-1α, which is unaffected by BMP-2 stimulation. (D) Immunogold electron microscopy analysis of BRII in C2C12 cells stably expressing HA-BRII-LF. BRII-LF was labeled as described in Materials and Methods, using secondary antibodies conjugated with 12-nm colloidal gold. For images I and II, cells were treated with antibodies before fixation and embedding. BRII-LF is observed at the cell surface (I) or in vesicles, which were identified as CCV (II). For images III to V, cell pellets were fixed and embedded before antibody application. BRII-LF is located in clusters of 50 to 75 nm in diameter. In images IV and V, sections were additionally incubated with an antibody which recognizes endogenous cav-1α, followed by secondary antibody conjugated with 6-nm colloidal gold. BRII-LF (arrows) is located in clusters together with cav-1α (arrowheads), indicating the localization of BRII in caveolae/caveosomes. Bar, 100 nm. IP, immunoprecipitation; WB, Western blotting.

Endogenously expressed cav-1α was immunoprecipitated from C2C12 cells stably expressing HA-tagged BRII-LF or BRII-SF. Figure 2A (Western blotting using anti-HA) demonstrates that both BRII-LF and -SF interact with cav-1α. To map the potential interaction site, the coprecipitation studies were repeated with BRII-TC1, a truncation mutant of BRII with a short, cytoplasmic tail that lacks the entire kinase domain (45). BRII-TC1 did not associate with cav-1α (Fig. 2B). One possi-

ble explanation is that the interaction site of cav-1α with BRII lies between amino acids 202 and 501, i.e., within the kinase domain of this receptor. Stimulation with BMP-2 shows no effect on the interaction of receptors with cav-1α (Fig. 2A and B). BRIa (data not shown) and BRIb (Fig. 2C) were also coimmunoprecipitated with cav-1α. Association of cav-1α with BRIb was observed in the absence of ligand and is not affected by the addition of BMP-2 (Fig. 2C). Furthermore, BRII was immunogold labeled in C2C12 cells stably expressing HA-tagged BRII at 4°C and its localization was analyzed by electron microscopy. Under noninternalizing conditions using a preembedding labeling method, receptors were detected predominantly at the cell surface and to a minor degree in invaginations, which were identified as clathrin-coated vesicles (CCVs) (Fig. 2D, panels I and II). CCVs are distinguishable by their ciliated border and also their size, which was found to be mostly around 100 nm in C2C12 cells (Fig. 2D, panel II). In additional experiments, a postembedding labeling method was applied to cell pellets. Here, BRII was accumulated in clusters of 50 to 75 nm in diameter (Fig. 2D, panel III). However, it was not possible to identify vesicles because of the method applied in these experiments. Therefore, we performed double-label immunogold electron microscopy and verified the colocalization of BRII and cav-1α by observing BRII in cav-1α-containing clusters, which were 50 to 75 nm in diameter (Fig. 2D, panels IV and V). From that, we conclude that BRII is localized in both CCPs/CCVs and smaller vesicles containing cav-1α, i.e., caveolae/caveosomes.

BMP receptors undergo constitutive endocytosis. To study BMP receptor endocytosis, extracellularly HA-tagged BRIb or myc-tagged BRII-LF (HA-BRIb, myc-BRII-LF [17]) was transfected into COS7 cells. Live cells were labeled at 4°C (to allow only extracellular surface labeling) with anti-HA or anti-myc antibodies, followed by incubation with fluorescent monovalent goat anti-mouse Fab′ fragments. Internalization was initiated by shifting the cells to 37°C for different periods. Typical images are depicted in Fig. 3A for HA-BRIb; similar results (not shown) were obtained for myc-BRII-LF. The initial distribution of both receptors prior to their being warmed to 37°C was homogeneous, characteristic for cell surface labeling. Incubation at 37°C resulted in a time-dependent shift to a vesicular pattern typical of endocytic vesicles (Fig. 3A). Clear vesicular staining was detected already after 5 min at 37°C, with longer incubation leading to larger vesicles, which concentrated in the perinuclear region. The intracellular nature of the vesicular staining was validated by acid stripping to remove noninternalized fluorescent antibodies from the cell surface (Fig. 3A, panel marked 30 min+stripping); this treatment removed the membrane-associated uniform staining but not the vesicular labeling.

In order to quantify the internalization rates of BRIb and BRII-LF, we measured the endocytosis of the receptors by the point confocal method described by us earlier (see Materials and Methods and reference 13). This method measures the level of antibody-labeled receptors remaining at the cell surface as a function of the incubation time at 37°C. Typical locations of measurement (laser focus spots) on a cell are shown in Fig. 3A (panel marked 20 min). The results for HA-BRIb expressed in COS7 cells are depicted in Fig. 3B. A control experiment demonstrating that the dissociation of fluorescent Fab′ from the cell surface during the incubation is negligible is shown in Fig. 3C; in this experiment, cells were fixed with paraformaldehyde to eliminate endocytosis, quenched by excess glycine, and only then subjected to antibody labeling and incubation at 37°C as in the endocytosis experiments. As shown in Fig. 3B, HA-BRIb undergoes constitutive endocytosis with a half-life ($t_{1/2}$) of ~14 min. The endocytosis rate (fraction of the surface receptor population internalized per minute), as calculated from the initial linear part of the internalization curve, was 0.028 min^{-1}. These values are very close to those measured for the TGF-β type II receptor, the high-affinity receptor in the TGF-β system, with a $t_{1/2}$ of ~15 min and endocytosis rate of 0.022 min^{-1} (13). The endocytosis rate of myc-BRII-LF in COS7 cells was rather similar and only slightly higher (Fig. 3D), exhibiting a $t_{1/2}$ of ~10 min and an endocytosis rate of 0.025 min^{-1}. Similar endocytosis measurements were also conducted on C2C12 cells transfected with the same receptor constructs; the results (Fig. 3E and data not shown) were very close to those obtained with COS7 cells ($t_{1/2}$ values of 14 and 15 min for BRIb and BRII-LF, respectively). For both receptor types, inclusion of a ligand (50 nM BMP-2) before and during endocytosis had no significant effects on the $t_{1/2}$ values (Fig. 3, legend). In summary, we conclude that both types of BMP receptors undergo constitutive endocytosis at close rates resembling those of the TGF-β receptors and that there are basically no differences between the internalization rates of these receptors in COS7 and in C2C12 cells.

BRII-LF and BRIb are internalized through CCPs, but only BRII-LF also undergoes caveola-like endocytosis. To determine the relative importance of specific mechanisms for the internalization of BRIb and BRII-LF, we employed several pathway-specific inhibitors that interfere selectively with either caveola-like endocytosis or clathrin-dependent internalization through CCPs. To investigate whether caveola-like internalization may contribute to BRIb or BRII-LF internalization, we used two independent pharmacological inhibitors, nystatin and genistein, which disrupt caveola-like endocytosis by different mechanisms. Nystatin (55) is a sterol-binding agent that disassembles caveolae and cholesterol assemblies in the membrane; genistein is a tyrosine kinase inhibitor that inhibits specific phosphorylation of cav-1 (4, 38). Both agents were shown to selectively inhibit caveola-like endocytosis with no effects on CCP-mediated internalization (53). The effects of these treatments on the internalization of HA-BRIb and myc-BRII-LF in COS7 and C2C12 cells are shown in Fig. 4. In both cell types, HA-BRIb internalization, as measured by the point confocal method (13), was not inhibited significantly by either nystatin or genistein. On the other hand, both treatments significantly inhibited the internalization of myc-BRII-LF; at the 20-min time point, the amount of fluorescently labeled receptors remaining at the cell surface was ~80% of the time zero level in the presence of the inhibitors, compared to ~50% in untreated cells (Fig. 4B). We conclude that caveola-like internalization is negligible for BRIb but significant for BRII-LF.

To determine the dependence of the internalization of the BMP receptors on CCPs, we employed three independent treatments known to disrupt CCP-mediated endocytosis. These include hypertonic treatment, cytosol acidification, and CP. Incubation in hypertonic medium dissociates and alters the

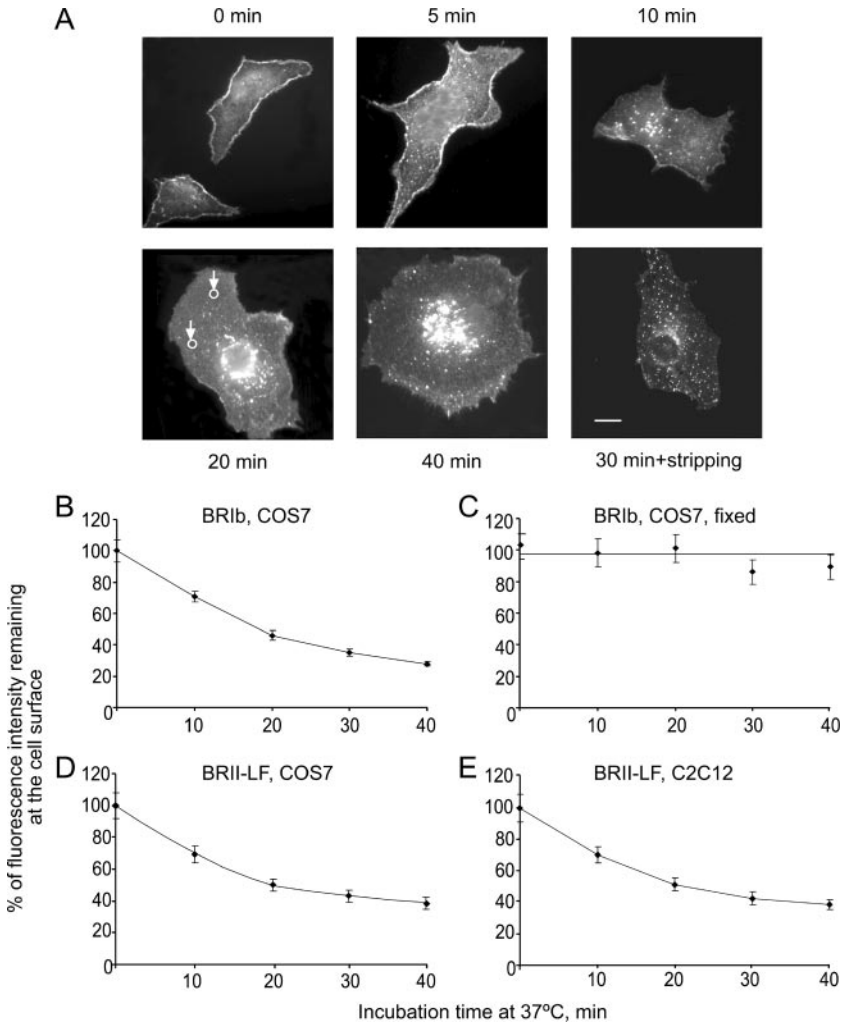

FIG. 3. Quantitative measurement of BMP receptor endocytosis. COS7 cells (A to D) or C2C12 cells (E) were transiently transfected with HA-BRIb (A to C) or myc-BRII-LF (D and E). After 48 h, live cells were labeled at 4°C with anti-HA or anti-myc IgG followed by Alexa 546 goat anti-mouse Fab′. After being washed, cells were incubated either at 4°C (time zero) or for the indicated periods at 37°C, shifted back to 4°C, and fixed. (A) Typical images of HA-BRIb in COS7 cells during endocytosis. As a control (A, lower rightmost panel), cells incubated at 37°C for 30 min were acid stripped to remove noninternalized fluorescent Fab′. Bar, 20 μm. (B to E) Quantitative measurements of BRIb and BRII-LF internalization. Measurements were done using the point confocal method (see Materials and Methods). (C) Control experiment where the cells were fixed with 4% paraformaldehyde in phosphate-buffered saline and quenched by three incubations with 50 mM glycine in phosphate-buffered saline prior to the labeling with antibodies, thus eliminating endocytosis and enabling the evaluation of the dissociation of the fluorescent antibodies from the surface during the incubation at 37°C (no significant dissociation occurred). The laser beam was focused on defined spots in the plasma membrane focal plane, away from vesicular staining (typical spots where the beam was focused are shown as white circles in the panel marked 20 min in panel A). The results shown at each time point are means ± standard errors of the means (SEM) of measurements for 80 to 150 cells. Addition of ligand (50 nM BMP-2; 1 h of preincubation at 4°C, keeping the ligand in during all subsequent incubations with antibodies and warming to 37°C) had no significant effects on the endocytosis rates of either receptor (data not shown).

clathrin lattices, while cytosol acidification freezes invaginated coated pits and prevents their being pinched off as CCVs (22, 27, 57). CP mediates redistribution of assembly protein complex-2 (AP-2) from the plasma membrane to endosomes (70, 72); it was shown to inhibit CCP-mediated endocytosis without affecting caveola-like internalization processes (53, 65). Typical images obtained in these experiments are depicted in Fig. 5A, and the average data of point confocal measurements are summarized in Fig. 5B. The results demonstrate that all the treatments that interfere with CCP-mediated endocytosis strongly inhibit the internalization of both BRIb and BRII-LF in either COS7 or C2C12 cells. Effective inhibition by CP was also observed following incubation with a lower concentration for a longer time (5 μM, 16 h), conditions employed for reporter gene assays in C2C12 cells (see Fig. 8B). We conclude that clathrin-dependent endocytosis is a major pathway for the internalization of both types of BMP receptors.

dyn2 plays a key role in the fission of vesicles like CCVs or caveosomes (26, 67). Overexpression of the dominant negative dyn2-K44A mutant protein is often used to inhibit endocytosis in general (69). As expected, overexpression of dyn2-K44A fully inhibited the endocytosis of both BMP receptors (Fig.

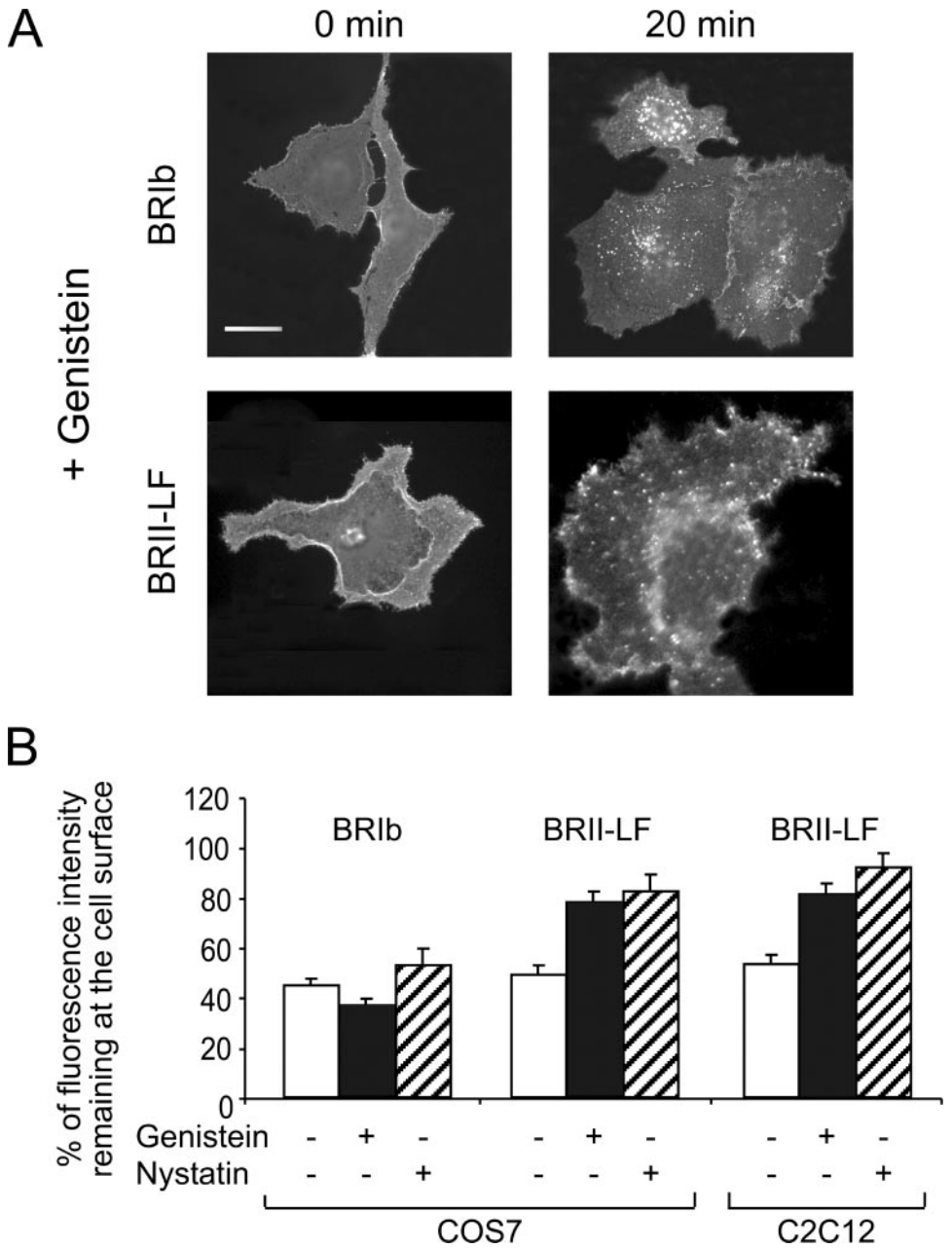

FIG. 4. Influence of inhibitors of caveola-like endocytosis on the internalization of BMP receptors. COS7 or C2C12 cells were transiently transfected with HA-BRIb or myc-BRII-LF as described for Fig. 3. After 48 h, they were incubated with nystatin (25 μg/ml, 30 min) or genistein (200 μM, 60 min) at 37°C. The surface receptors were then labeled at 4°C with fluorescent antibodies as for Fig. 3, followed by a 20-min incubation at 37°C or 4°C (control) in media containing inhibitors. Cell surface receptor levels were quantified by the point confocal method. (A) Typical images (COS7 cells) showing inhibition by genistein of the shift in HA-BRIb and myc-BRII-LF to vesicular endocytic patterns. Analogous results (not shown) were obtained with C2C12 cells or by using nystatin in place of genistein. Bar, 20 μm. (B) Quantification of the internalization studies. The reduction in cell surface labeling due to internalization was quantified by the point confocal method as described for Fig. 3. The fluorescence intensity in identically treated cells at time zero was taken as 100% for each treatment individually to eliminate the contribution of potential alterations in the steady-state surface levels of the receptors in the presence of the inhibitors. The results are means ± SEM of measurements of 80 to 140 cells in each case. In a comparison of the results from pairs of treated versus untreated cells for each group, neither genistein nor nystatin had significant effects on HA-BRIb internalization ($P > 0.05$, Student's t test); similar results (not shown) were obtained for HA-BRIb in C2C12 cells. However, both treatments had significant inhibitory effects on myc-BRII-LF internalization either in COS7 cells ($P < 10^{-12}$ for genistein and $P < 10^{-15}$ for nystatin) or in C2C12 cells ($P < 10^{-12}$ and $P < 10^{-17}$ for genistein and nystatin, respectively).

5B). It did not have significant effects on the cell surface levels of the BMP receptors relative to the levels in the absence of dyn2-K44A (changes were less than 5%), measured by the point confocal method following labeling with fluorescent antibodies of epitope-tagged BRIb or BRII-LF at the surfaces of cells cotransfected with the dynamin mutant and prefixed with paraformaldehyde prior to antibody labeling to prevent endocytosis (as for Fig. 3C; data not shown).

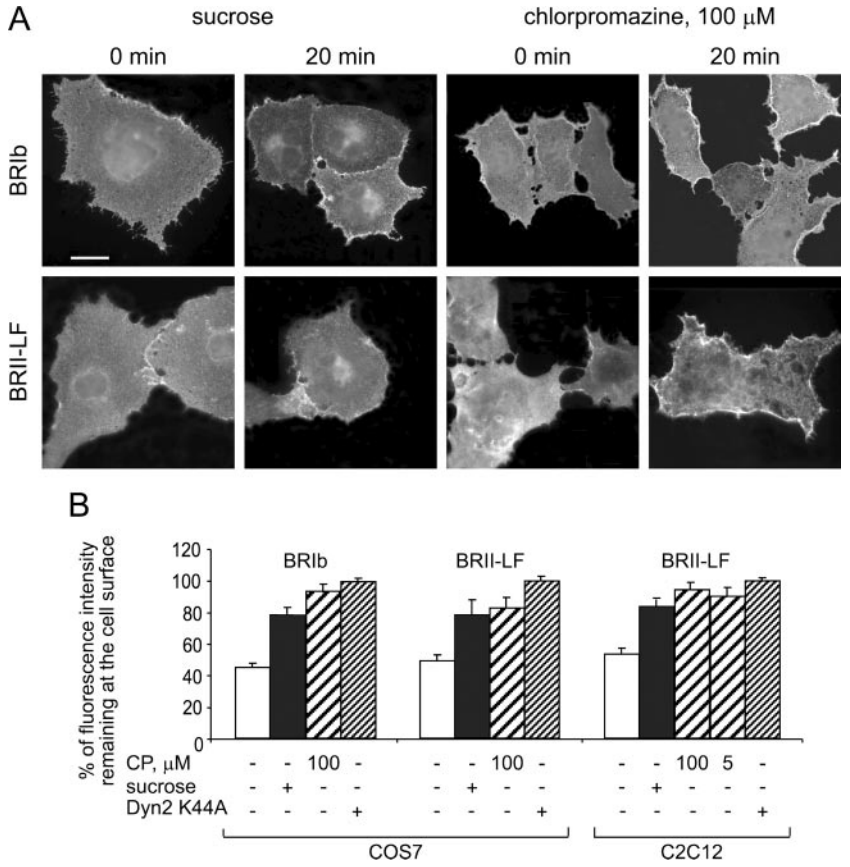

FIG. 5. Treatments that disrupt CCP-mediated endocytosis inhibit the internalization of BMP receptors. COS7 or C2C12 cells were transfected with HA-BRIb or myc-BRII-LF as described for Fig. 3. In some experiments, the cells were cotransfected with a sixfold excess of dyn2-K44A along with the BMP receptor construct. Hypertonic treatment, cytosol acidification, and treatment with CP were employed as described in the text. (A) Typical images of the effects of hypertonic treatment (sucrose) or CP (100 μM, 15 min) on the endocytosis of HA-BRIb and myc-BRII-LF in COS7 cells. Similar levels of inhibition were observed following cytosol acidification (data not shown), as well as in cells cotransfected with dyn2-K44A and in C2C12 cells (see panel B). Bar, 20 μm. (B) Quantification by the point confocal method. The fluorescence intensity measured at time zero on similarly treated cells was taken as 100% for each specific treatment. Bars represent means ± SEM of measurements conducted on 80 to 140 cells in each case. A comparison of pairs on treated versus untreated cells demonstrates highly significant effects of all the treatments on both COS7 and C2C12 cells ($P < 10^{-12}$ and in some cases $P < 10^{-25}$). Analogous results (not shown) were obtained for BRIb in C2C12 cells.

Cholesterol depletion has distinct effects on BMP-2 signaling. To examine the influence of cholesterol-dependent plasma membrane regions on signaling, we performed cholesterol depletion experiments by metabolic inhibition of cholesterol synthesis in the presence of LPDS using lovastatin and a low concentration of mevalonate (31, 37). The conditions employed (see Materials and Methods) resulted in depletion of the cholesterol level by 30 to 33% in both COS7 and C2C12 cells (data not shown). These levels of cholesterol depletion were shown to be sufficient to disrupt the association of specific proteins with rafts in cell membranes (44, 62).

At first we studied the impact of cholesterol depletion on the level of phosphorylated Smad1/5. Western blot analyses using a specific antibody show that Smad1/5 phosphorylation is not affected by cholesterol depletion (Fig. 6A). To further investigate signaling downstream of Smad1/5 phosphorylation, we examined whether cholesterol depletion altered the BMP-mediated transcriptional response by the use of reporter genes. BRE luciferase assays (35) revealed that also the continuation of BMP signaling is almost unaffected by lovastatin, exhibiting only a 10% decrease in BMP-2-dependent transcriptional activity (Fig. 6B).

To explore whether the production of ALP, which depends on Smad-independent signaling, is influenced by cholesterol depletion, ALP assays were performed. Treatment with lovastatin reduced both the mRNA level (Fig. 6C) and ALP production (Fig. 6D) by 80% and 75%, respectively, suggesting an influence of cholesterol-enriched membrane regions on Smad-independent signaling.

In summary, we found that lovastatin does not inhibit the phosphorylation of Smad1/5 or the activation of the Smad-dependent transcriptional response, although it disrupts rafts/caveolae. However, lovastatin selectively inhibits the BMP-2-induced Smad-independent pathway.

Induction of caveola formation at the cell surface decreases BMP signaling via Smads. Previously, it was shown that overexpression of cav-1 leads to de novo synthesis or increased numbers of caveolae at the cell surface but that caveola-mediated endocytosis via caveosomes is not enhanced (15, 59). By investigating the level of phosphorylated Smad1/5 after BMP-2

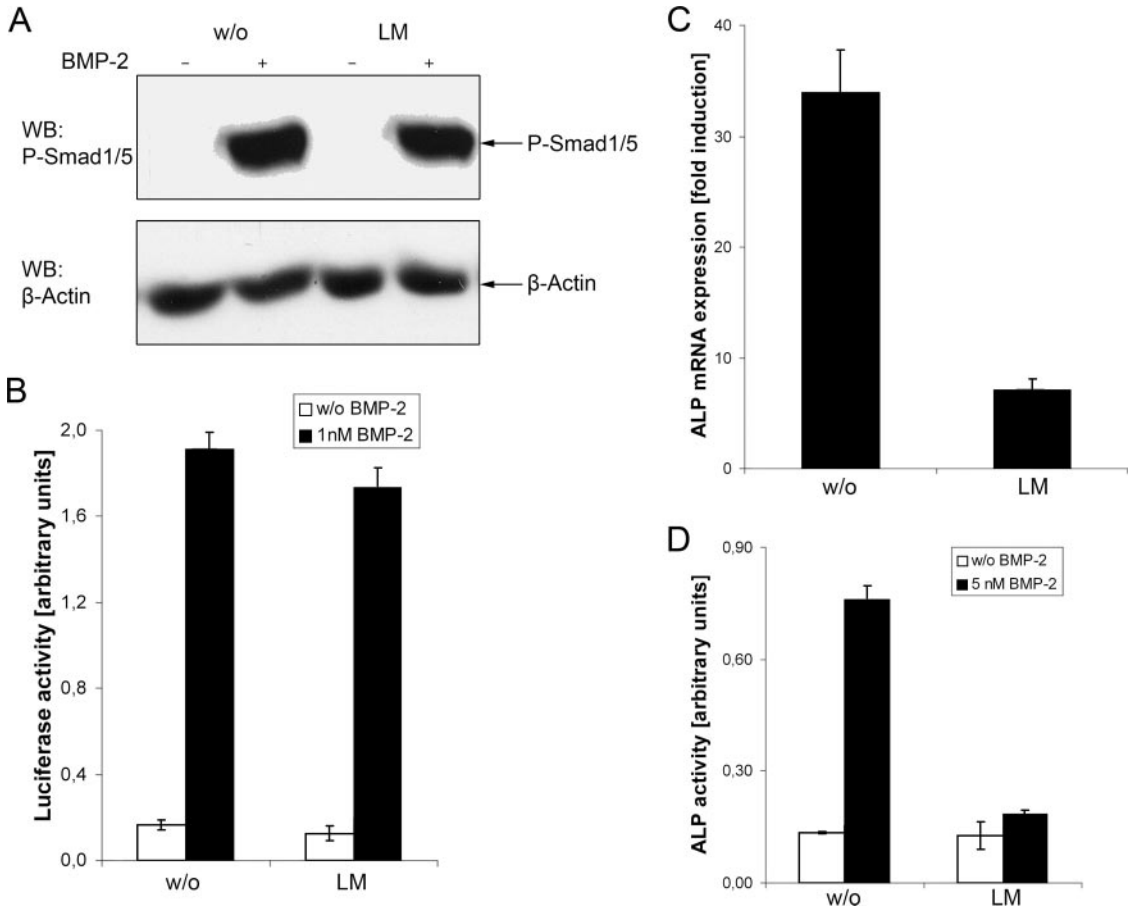

FIG. 6. Influence of cholesterol-enriched plasma membrane regions on BMP signaling pathways. C2C12 cells were treated with 50 μM lovastatin and 50 μM mevalonate and stimulated with BMP-2 as described in the text. (A) Western blot (WB) analyses using an anti-phospho-Smad1/5 (P-Smad1/5) antibody show that Smad1/5 phosphorylation is not altered by LM. For a loading control, the membrane was incubated with anti-β-actin antibody. (B) C2C12 cells were transfected with $p(BRE)_4$-luc and pRLTK before metabolic inhibition using LM was accomplished. BMP signaling is only slightly reduced by LM. Error bars represent standard deviations from three different assays. (C) RT-PCR of ALP expression levels shown as the level of induction (*n*-fold) upon BMP-2 stimulation; cholesterol depletion by LM results in a reduction of the ALP transcript by 80%. Error bars represent standard deviations (SD) from duplicates. The experiment was done two times. (D) ALP activity measurements after cholesterol depletion by LM (this experiment was performed in parallel with the experiment whose results are shown in panel C) show reduction by 75%. Error bars represent SD from two independent experiments, each with triplicates. w/o, without.

stimulation in C2C12 cells, we saw no differences, regardless of whether cav-1 was overexpressed or not (Fig. 7A). From this, we conclude that BMP-2-induced Smad1/5 phosphorylation occurs independently of caveola formation.

Furthermore, we show that the BMP-mediated reporter gene response is significantly reduced when cav-1α was transfected (Fig. 7B). To verify that this effect relies on signaling via BMP receptors, we additionally cotransfected BRII and BRIa to cav-1α. BMP-2 signaling was increased when BRIa, BRII, or both receptor types were transfected. This effect was abrogated when cav-1α was cotransfected (Fig. 7B), suggesting that the continuation of BMP-Smad signaling is not also mediated by caveolae, but caveolae rather resemble structures which trap the receptors from their signaling compartment.

To further address the effect of caveolae on Smad phosphorylation, we performed siRNA experiments to downregulate endogenous cav-1 in C2C12 cells. As controls, we transfected an empty vector and a fluorescently labeled nontargeting siRNA. Western blot analyses showed ~90%-decreased cav-1α expression when cav-1-specific siRNA was transfected (Fig. 7C, upper panel). However the phosphorylation of Smad1/5 is not affected by a reduced cav-1 expression (Fig. 7C, bottom panel), demonstrating again that this step in BMP signaling occurs independently of cav-1, i.e., caveola formation.

Inhibition of endocytosis by the dyn2-K44A mutant has no impact on BMP-induced Smad phosphorylation. To verify the independence of Smad1/5 phosphorylation from endocytosis, we transfected C2C12 cells with wt dyn2 or the K44A mutant dyn2. Western blot analyses revealed no significant differences in the levels of phosphorylated Smad1/5 between dyn2-K44A and wt dyn2 or when an empty vector was transfected (Fig. 7D). This result indicates that BMP-2-mediated Smad1/5 phosphorylation is triggered while the receptors are at the plasma membrane.

Influence of CCP-mediated endocytosis on BMP signaling. Likewise, we investigated the effect of CP on different steps of BMP signaling. In dose-response experiments, we show that

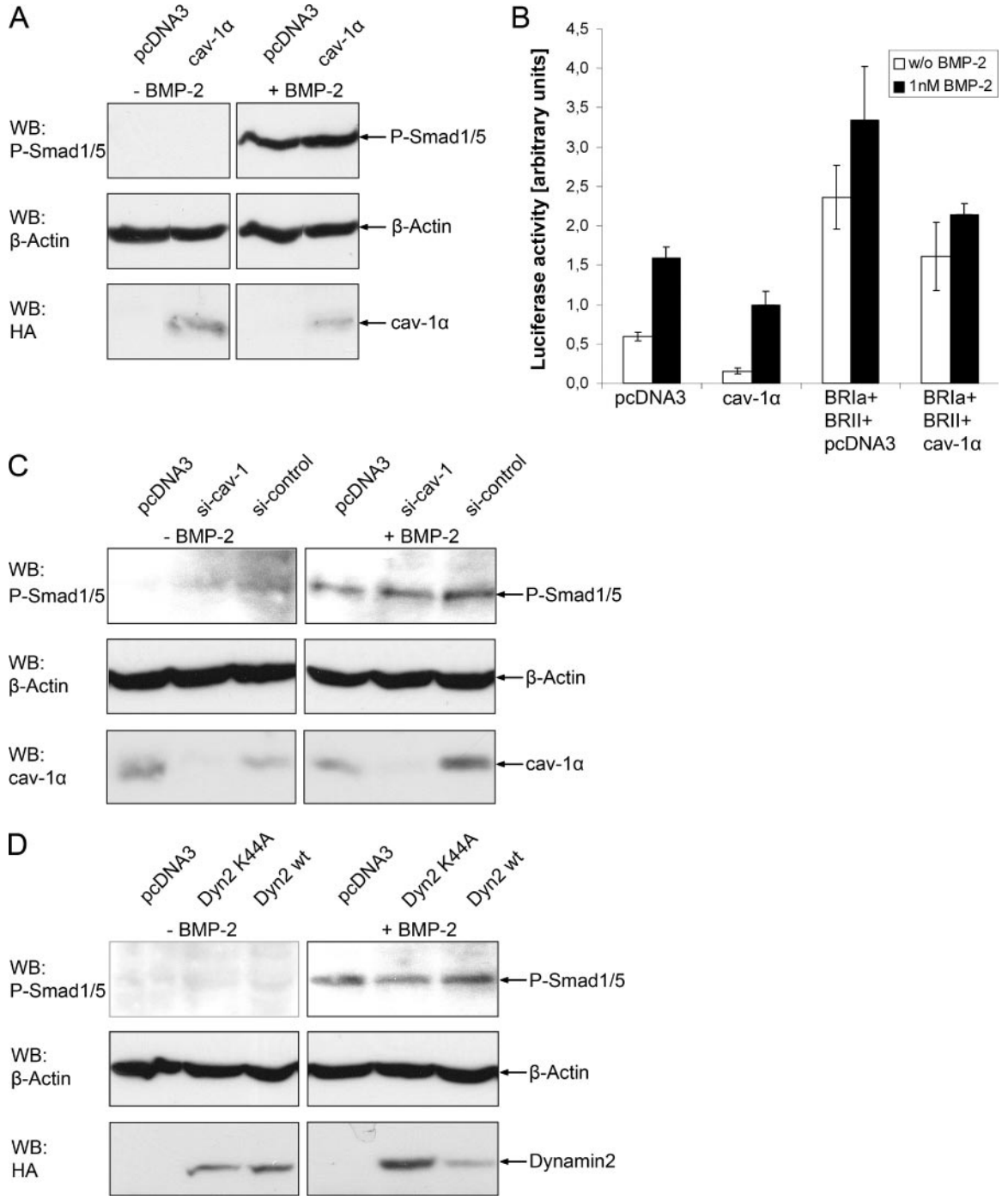

FIG. 7. Effect of cav-1α, cav-1-siRNA, or wt dyn2 and -K44A expression on BMP signaling. (A) C2C12 cells were transfected with HA-tagged cav-1α and stimulated with 20 nM BMP-2 for 30 min. Western blot analyses using anti-P-Smad1/5-specific antibodies reveal no significant change in Smad1/5 phosphorylation. For a loading control, the same membrane was incubated with anti-β-actin antibody. (B) Cells were transiently transfected with cav-1α, BRII-LF, and BRIa as indicated, together with reporter constructs. cav-1α expression significantly reduced both ligand-independent and -dependent BMP signaling. Error bars represent standard deviations from three different assays. (C) cav-1-specific siRNA was transfected in C2C12 cells to knock down endogenous cav-1 expression. A P-Smad1/5 Western blot shows no influence of cav-1 downregulation on the phosphorylation level. (D) Expression of HA-tagged wt dyn2 and the dyn-K44A mutant shows no significant alteration in the level of phosphorylated Smad1/5. Controls confirm wt dyn2, dyn2-K44A, and β-actin expression. WB, Western blotting; w/o, without.

both conditions, incubation with a low CP concentration, i.e., 5 μM for 16 h, and a high CP concentration, i.e., 100 μM for 30 min, were efficient in blocking the endocytosis of BRII in C2C12 cells (Fig. 5B).

By investigating the phosphorylation of Smad1/5, we found that CP does not affect this initial step of Smad signaling (Fig. 8A). Furthermore, we examined whether the continuation of BMP-initiated signaling is influenced by CP

treatment. Therefore, we accomplished BRE reporter gene assays while specifically inhibiting CCP-mediated endocytosis. As seen in Fig. 8B, BMP signaling is decreased by 65% after CP treatment. Therefore, we conclude that, while the transcriptional response on BMP signaling is dependent on CCP-mediated endocytosis, the phosphorylation of Smad1/5 is not affected by this endocytic process. Moreover, we investigated the effect of CP on ALP production. Here, we observed that the production of functional ALP was reduced by around 80% after CP treatment (Fig. 8C). Taking our previous results into consideration (Fig. 6C), we conclude that the BMP-2-mediated induction of ALP is dependent both on Smad-dependent and on Smad-independent signaling.

BRII is associated with Eps15R, a constituent component of CCPs. Recently, we performed a proteomics-based approach to identify BRII-associated proteins (23). Eps15R, a protein which constitutively resides in CCPs (8, 52), was found to interact with the cytoplasmic domain of BRII. Here, we confirm this interaction by coimmunoprecipitation using anti-Eps15R antibody. For this, 293T cells were transfected with HA-tagged BRII and enhanced green fluorescent protein (EGFP)-tagged Eps15R. After immunoprecipitating the receptor via its HA tag, Eps15R is detected in the precipitate by Western blotting with an EGFP antibody (Fig. 9A). The experiment was repeated during the expression of truncation mutants of BRII to map the potential binding site of Eps15R at BRII. Here, Eps15R was precipitated by using an Eps15R-specific antibody and the receptor variants were detected in the precipitate via HA antibody. BRII-SF and BRII-TC1 interact with Eps15R (Fig. 9B). This suggests that one Eps15R-BRII interaction site resides at the 27-amino-acid (aa) juxtamembrane domain of the receptor (aa 176 to 202). Since Eps15R was identified by glutathione *S*-transferase pulldown experiments using the 537 residues of the cytoplasmic tail of BRII (aa 502 to 1038) (see Fig. SA3 in the supplemental material), a second binding site of Eps15R to BRII is proposed.

DISCUSSION

The endocytosis of growth factor receptors plays an important role in the activation and propagation as well as the attenuation of signaling pathways (41). It is also one of the key processes in several pathologies; e.g., it controls the level of receptors at the cell surface (16, 66).

Recently, it was shown that TGF-β and epidermal growth factor signaling pathways depend on endocytic events and vesicles. In this context, CCPs and early endosomes are described to be the signaling compartments, but caveolae and caveosomes seem to represent sites where signaling is downregulated or attenuated (10, 11, 24).

Here, we report the localization of BMP receptors in distinct membrane domains, their endocytosis, and their consequential impact on BMP signaling. We demonstrated that BRI and BRII reside in both DRM domains and CCPs and that both membrane regions influence BMP signaling in distinct ways.

First, we showed that BRI and BRII reside in DRMs and cofractionate with cav-1α (Fig. 1). Moreover, in cells which do not exhibit caveolae due to a lack of cav-1 expression, BMP receptors are still included in DRM fractions (Fig. 1A and D). These findings suggest that BMP receptors are present in

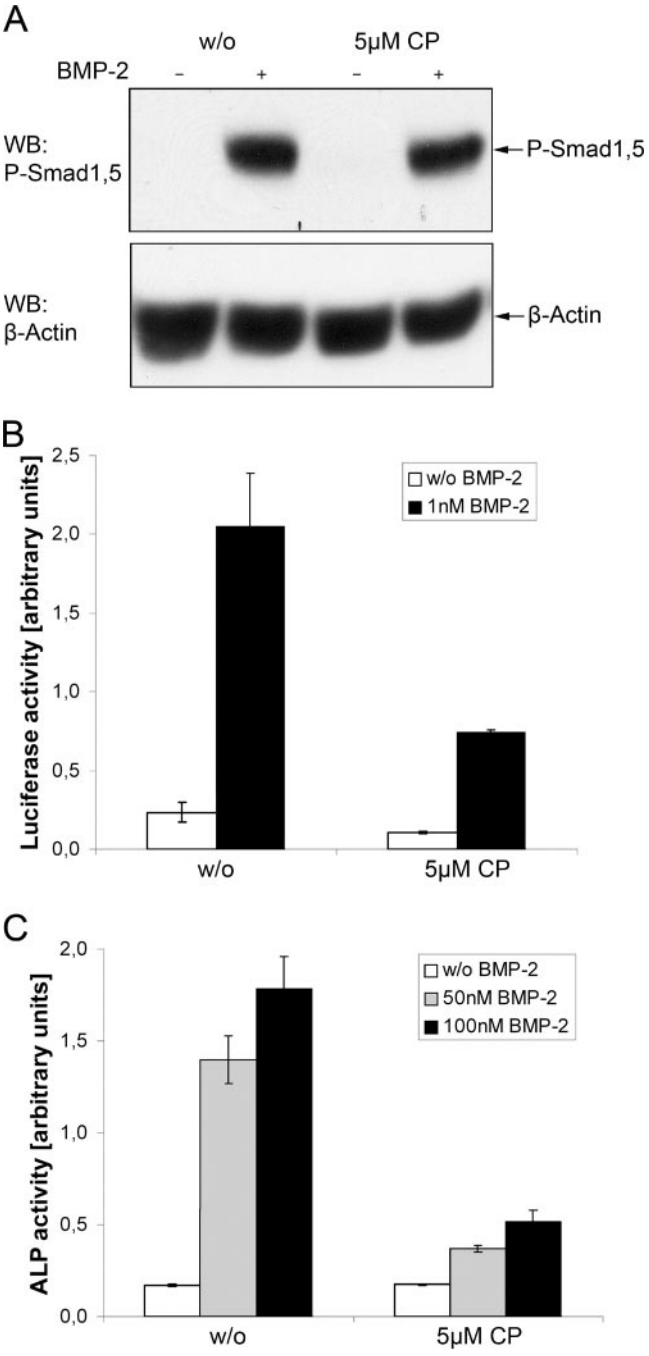

FIG. 8. Influence of CP on BMP signaling. C2C12 cells were treated with 5 μM CP and stimulated with BMP-2 as described in the text. (A) Western blot analyses with anti-P-Smad1/5 antibody show that the level of phosphorylated Smad1/5 was not altered by CP treatment. The loading control is shown by anti-β-actin antibody (lower panel). (B) C2C12 cells were transfected with $p(BRE)_4$-luc and pRLTK and treated with CP. This results in a 65%-reduced BMP response. Error bars represent standard deviations (SD) from three different assays. (C) ALP activity was measured after CCP-mediated endocytosis was blocked by CP. This treatment reduces ALP activity by around 80%. Error bars represent SD from three different assays. WB, Western blotting; w/o, without.

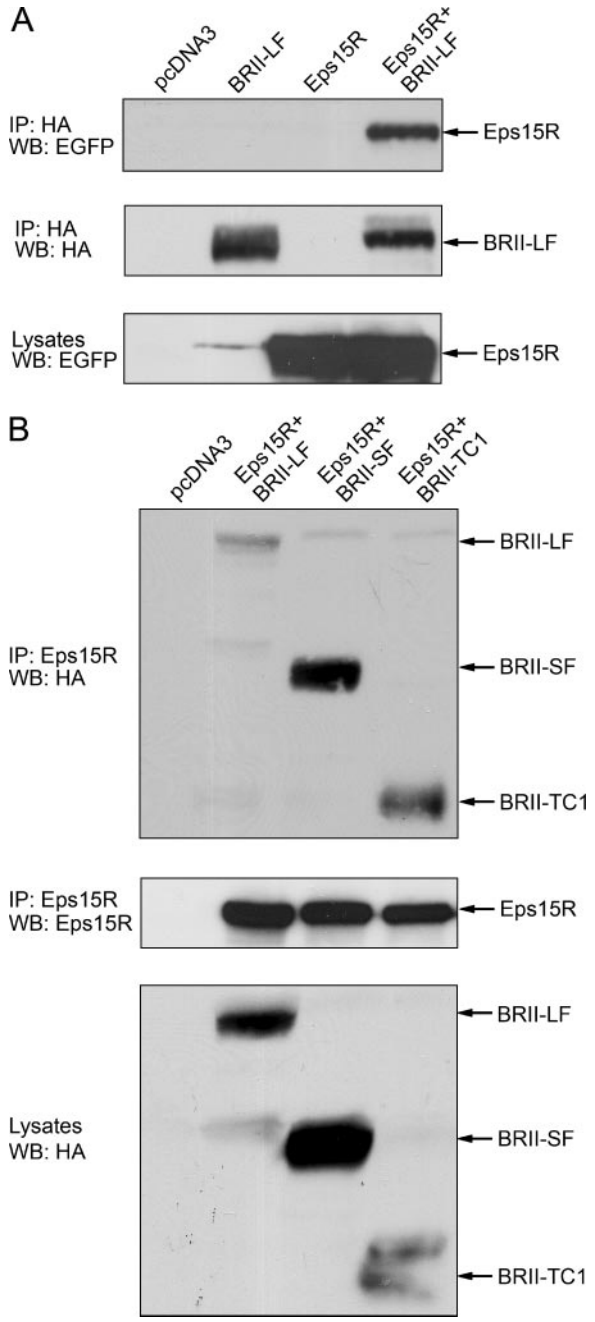

FIG. 9. Association of BRII with Eps15R. 293T cells were transfected with HA-tagged BRII-LF, BRII-SF, or BRII-TC1 and EGFP-tagged Eps15R. Immunoprecipitation (IP) and Western blotting (WB) were accomplished as indicated in the text. (A) Eps15R and BRII-LF form a complex in 293T cells. (B) All receptor variants are verified in the Eps15R precipitate with HA antibody. Eps15R interacts also with BRII-TC1.

caveolae and/or noncaveolar DRMs. Support for an association of BMP receptors with caveolae in C2C12 cells was provided by coimmunoprecipitation and immunogold electron microscopy studies (Fig. 2). We showed that BRI and BRII interact with endogenously expressed cav-1α (Fig. 2A and C) and colocalize with cav-1α in clusters of the size of caveolae (Fig. 2D, panels IV and V). Sequence analyses of BMP type I receptors revealed a cav-1 consensus motif (9) in the kinase domain (YSFGLILW with respect to aa 401 to 408 in BRIb and YSFGLIIW with respect to aa 431 to 438 in BRIa), which confirms our finding of a strong association between cav-1α and type I receptors (Fig. 2C) as well as the high occurrence of BRI in DRM fractions (Fig. 1A and B). The interaction of BRII and cav-1α requires the kinase domain of BRII, because BRII-SF is able to bind cav-1α, whereas BRII-TC1, a truncation mutant lacking the kinase domain, fails to bind cav-1α (Fig. 2A and B). Sequence analyses of the BRII cytoplasmic region showed no correlation with the cav-1 binding site (9), suggesting an association via an alternative mechanism. Since we could show previously that BRII-TC1 is too short to form PFCs with BRI (45), the observed coimmunoprecipitation of BRII with cav-1 might be indirect via the associated BRI.

With respect to the proposed localization of BMP receptors in caveolae/DRMs, we studied their mode of endocytosis in more detail. The results point to a constitutive internalization of the receptors (Fig. 3), while the kinetics of the internalized receptors (Fig. 3B) parallels those measured for the TGF-β receptors (13). Investigating the effects of inhibitors of caveola- and raft-dependent endocytosis on the internalization of BMP receptors, we found that, while BRIb was internalized regardless of whether nystatin or genistein was present or not, BRII internalization was blocked efficiently by the same treatments (Fig. 4). This finding suggests a contribution of cholesterol-dependent endocytosis on the internalization of BRII but not of BRIb.

Next we analyzed the classical clathrin-mediated endocytosis pathway. Using inhibitors to specifically block this route, we could show that the endocytosis of both types of BMP receptors was inhibited (Fig. 5).

In summary, we found that BRII is internalized through both CCP- and caveola/DRM-mediated endocytic mechanisms but that BRIb is internalized exclusively through CCPs.

To investigate the contribution of BMP receptor localization in distinct regions of the plasma membrane and of receptor endocytosis on BMP signaling, we studied how Smad-dependent and Smad-independent BMP signaling pathways are altered, while intervening in endocytosis.

To disrupt DRM regions and caveolae, the method of metabolic inhibition of cholesterol synthesis using lovastatin was applied (31, 37). We could show that lovastatin, although it disrupts rafts/caveolae, did not inhibit the BMP-2-mediated phosphorylation of Smad1/5 (Fig. 6A) or transcriptional activity via Smads (BRE-reporter gene assay) (Fig. 6B). From this, we propose that the entire Smad pathway is insensitive to cholesterol depletion. However, the BMP-2-mediated induction of the ALP transcript and ALP protein activity is strongly sensitive to lovastatin treatment (Fig. 6C and D), suggesting that a Smad-independent pathway initiates from BMP receptors localized in cholesterol-enriched plasma membrane regions.

It was reported that cav-1 overexpression leads to the formation of more caveolae at the cell surface; however, endocytosis via these plasma membrane invaginations is blocked (59). We show that while Smad1/5 phosphorylation was unaffected upon cav-1α overexpression, the Smad-dependent transcriptional activity in response to BMP-2 was significantly reduced (Fig. 7A and B). This leads to the conclusion that caveolae

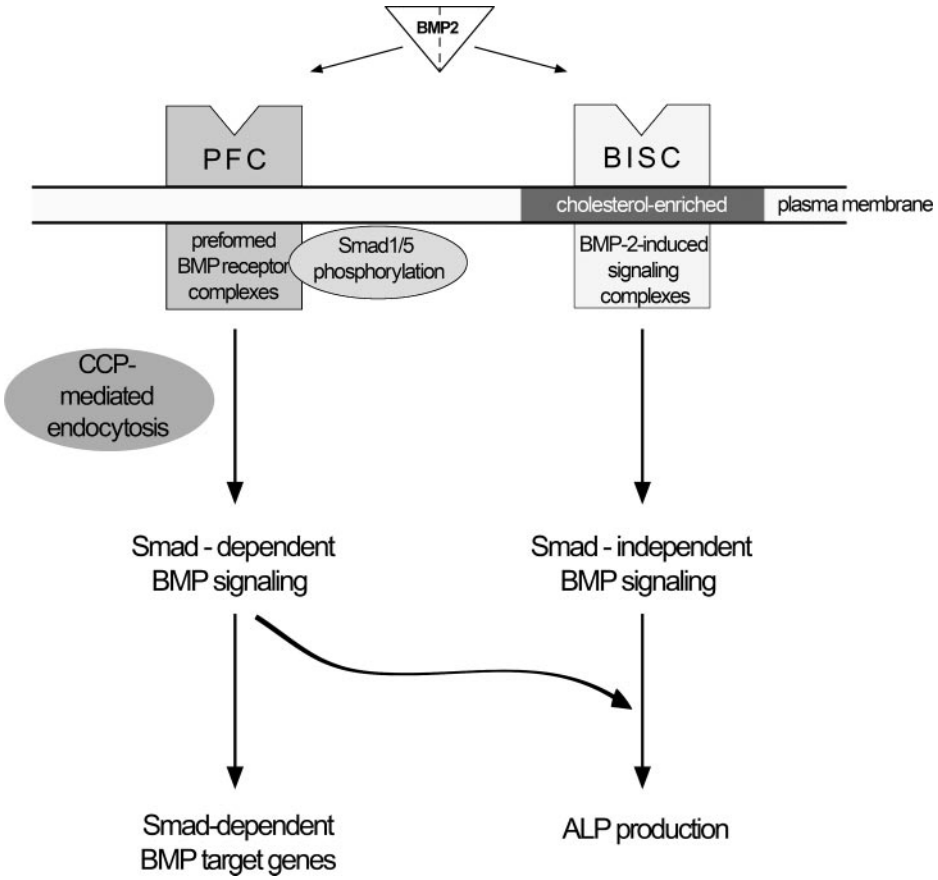

FIG. 10. Smad-dependent signaling and Smad-independent BMP signaling originate from distinct endocytic routes of the BMP receptors. Smad-dependent signaling is initiated upon BMP-2 binding to PFCs, which exist in an inactive state at the cell surface prior to ligand binding (45). Activation of this signaling cascade by BMP-2 binding results in the phosphorylation of Smad1/5 by the type I receptor. This step in Smad signaling occurs while the receptors reside at the plasma membrane; inhibition of endocytosis (treatment with chlorpromazine or expression of dominant negative dynamin) does not affect BMP-2-mediated Smad phosphorylation. Subsequent endocytosis of the receptors through CCPs, however, is needed to transmit the Smad signal into the nucleus to control the transcriptional activity of target genes. Treatment with lovastatin to perturb cholesterol-dependent plasma membrane regions does not affect Smad signaling but reduces BMP-2-mediated ALP induction through a Smad-independent cascade. This signaling pathway is initiated by the binding of BMP-2 to high-affinity BRI, and a subsequent recruitment of BRII into the signaling receptor complex BISC occurs (45). From the data presented here, we conclude that Smad-independent signaling resulting in ALP induction starts from receptors (BISCs) residing in cholesterol-enriched plasma membrane regions.

might represent compartments where BMP receptors certainly reside but where BMP-Smad signaling is abrogated by trapping the receptors from their actual signaling compartments. Others have shown that caveolae and caveosomes resemble sites where TGF-β receptors are degraded, and therefore signaling is retarded (11).

We clearly demonstrate here that caveolae are not required for BMP-2-mediated Smad1/5 phosphorylation, as cav-1α overexpression and also cav-1 knockdown by specific siRNA did not alter the phosphorylation level (Fig. 6A and D).

Taking our previous findings into consideration (45), we can conclude that BMP-Smad signaling induced at PFCs is independent of raft/caveola association. On the other hand, signaling initiated at BISCs, which leads to Smad-independent signaling, is reliant on the association of BMP receptors with rafts and caveolae (Fig. 10).

Next, we applied the inhibition of both caveola- and clathrin-mediated endocytosis to investigate its impact on Smad signal transduction. Dynamin2 is a GTPase that regulates CCP assembly as well as late events in CCV and caveosome formation (26, 71). We demonstrated here that blocking dynamin2 action by using dominant negative dyn2-K44A had no impact on BMP-mediated Smad1/5 phosphorylation (Fig. 7D) but that receptor endocytosis was completely blocked by this mutant (Fig. 5B). This result indicates that Smad1/5 is phosphorylated independently of endocytic events at the plasma membrane.

To further address CCP-mediated endocytosis, we employed inhibition of this pathway by CP. While CP blocks endocytosis of the BMP receptors (Fig. 5), BMP-mediated Smad1/5 phosphorylation was unaffected (Fig. 8A), suggesting again that this initial step in Smad signaling occurs while the receptors are still present at the plasma membrane. However, CP treatment results in a strong reduction of Smad-dependent transcription (Fig. 8B). The same was observed when ALP was measured after stimulation with BMP-2 (Fig. 8C), proving that ALP induction requires, besides the Smad-independent pathway (induced by BISCs [45]), a Smad-dependent cascade. Also, signaling via TGF-β receptors along the Smad pathway was

reported to occur mainly via CCPs and on the early endosomal membrane. But while some publications favor an impact of endocytic events on Smad2/3 phosphorylation (11, 24, 50), others report endocytosis-independent Smad2/3 phosphorylation (39, 56). However, the results presented in our study concerning BMP signaling clearly conclude that Smad1/5 is phosphorylated at the plasma membrane—independently from cav-1 (Fig. 7A and C)-, clathrin (Fig. 8A)-, and dynamin2-mediated endocytosis (Fig. 7D) as well as a cholesterol-sensitive membrane environment (Fig. 6A).

In addition, we found BRII localized in CCPs/CCVs using immunogold electron microscopy (Fig. 2D) and associated with Eps15R (Fig. 9). Eps15R is a protein related to Eps15 and epsin, which play an important role in the clathrin-mediated endocytosis of growth factor receptors (33). They function as adaptors between ubiquitinated membrane cargo and the clathrin coat or other endocytic scaffolds (51). Therefore, the interaction between BRII and Eps15R represents a new link between the BMP signaling network and endocytic/trafficking events inside the cell.

Taken together, our data imply that BMP-2-induced signal transduction is compartmentalized into an early part, the phosphorylation of Smad1/5, which takes place independently of endocytosis at the cell surface and a subsequent signaling cascade. Here, the Smad-dependent signaling pathway is dependent on a functional CCP-mediated endocytosis, whereas Smad-independent pathways, resulting in the production of ALP, rely on the association of caveolae/DRMs with the receptor complexes (Fig. 10).

ACKNOWLEDGMENTS

We thank Georg Krohne for advice on electron microscopy and Ernst Conzelmann for assistance during lipid chromatography. We are especially grateful to the excellent technical support of Nadine Yurdagül-Hemmrich. We thank Walter Sebald for recombinant BMP-2 and helpful discussions.

This work was supported in part by grants from the DFG (Kn332/8-1 to P.K.), from the Israel Science Foundation (grant 185/05), and from the Israel Cancer Research Fund (to Y.I.H.). Y.I.H. holds the Zalman Weinberg Chair in Cell Biology.

REFERENCES

1. **Anderson, R. G.** 1998. The caveolae membrane system. Annu. Rev. Biochem. **67:**199–225.
2. **Anderson, R. G., and K. Jacobson.** 2002. A role for lipid shells in targeting proteins to caveolae, rafts, and other lipid domains. Science **296:**1821–1825.
3. **Anderson, R. G., B. A. Kamen, K. G. Rothberg, and S. W. Lacey.** 1992. Potocytosis: sequestration and transport of small molecules by caveolae. Science **255:**410–411.
4. **Aoki, T., R. Nomura, and T. Fujimoto.** 1999. Tyrosine phosphorylation of caveolin-1 in the endothelium. Exp. Cell Res. **253:**629–636.
5. **Brown, D. A., and E. London.** 2000. Structure and function of sphingolipid- and cholesterol-rich membrane rafts. J. Biol. Chem. **275:**17221–17224.
6. **Canalis, E., A. N. Economides, and E. Gazzerro.** 2003. Bone morphogenetic proteins, their antagonists, and the skeleton. Endocr. Rev. **24:**218–235.
7. **Ceresa, B. P., and S. L. Schmid.** 2000. Regulation of signal transduction by endocytosis. Curr. Opin. Cell Biol. **12:**204–210.
8. **Coda, L., A. E. Salcini, S. Confalonieri, G. Pelicci, T. Sorkina, A. Sorkin, P. G. Pelicci, and P. P. Di Fiore.** 1998. Eps15R is a tyrosine kinase substrate with characteristics of a docking protein possibly involved in coated pits-mediated internalization. J. Biol. Chem. **273:**3003–3012.
9. **Couet, J., S. Li, T. Okamoto, T. Ikezu, and M. P. Lisanti.** 1997. Identification of peptide and protein ligands for the caveolin-scaffolding domain. Implications for the interaction of caveolin with caveolae-associated proteins. J. Biol. Chem. **272:**6525–6533.
10. **Di Fiore, P. P., and P. De Camilli.** 2001. Endocytosis and signaling. An inseparable partnership. Cell **106:**1–4.
11. **Di Guglielmo, G. M., C. Le Roy, A. F. Goodfellow, and J. L. Wrana.** 2003. Distinct endocytic pathways regulate TGF-beta receptor signalling and turnover. Nat. Cell Biol. **5:**410–421.
12. **Douglass, A. D., and R. D. Vale.** 2005. Single-molecule microscopy reveals plasma membrane microdomains created by protein-protein networks that exclude or trap signaling molecules in T cells. Cell **121:**937–950.
13. **Ehrlich, M., A. Shmuely, and Y. I. Henis.** 2001. A single internalization signal from the di-leucine family is critical for constitutive endocytosis of the type II TGF-beta receptor. J. Cell Sci. **114:**1777–1786.
14. **Evan, G. I., G. K. Lewis, G. Ramsay, and J. M. Bishop.** 1985. Isolation of monoclonal antibodies specific for human c-myc proto-oncogene product. Mol. Cell. Biol. **5:**3610–3616.
15. **Fra, A. M., E. Williamson, K. Simons, and R. G. Parton.** 1995. De novo formation of caveolae in lymphocytes by expression of VIP21-caveolin. Proc. Natl. Acad. Sci. USA **92:**8655–8659.
16. **Garuti, R., C. Jones, W. P. Li, P. Michaely, J. Herz, R. D. Gerard, J. C. Cohen, and H. H. Hobbs.** 2005. The modular adaptor protein autosomal recessive hypercholesterolemia (ARH) promotes low-density lipoprotein receptor clustering into clathrin-coated pits. J. Biol. Chem. **280:**40996–41004.
17. **Gilboa, L., A. Nohe, T. Geissendorfer, W. Sebald, Y. I. Henis, and P. Knaus.** 2000. Bone morphogenetic protein receptor complexes on the surface of live cells: a new oligomerization mode for serine/threonine kinase receptors. Mol. Biol. Cell **11:**1023–1035.
18. **Gilboa, L., R. G. Wells, H. F. Lodish, and Y. I. Henis.** 1998. Oligomeric structure of type I and type II transforming growth factor beta receptors: homodimers form in the ER and persist at the plasma membrane. J. Cell Biol. **140:**767–777.
19. **Goebel, J., K. Forrest, L. Morford, and T. L. Roszman.** 2002. Differential localization of IL-2- and -15 receptor chains in membrane rafts of human T cells. J. Leukoc. Biol. **72:**199–206.
20. **Goldstein, J. L., S. K. Basu, and M. S. Brown.** 1983. Receptor-mediated endocytosis of low-density lipoprotein in cultured cells. Methods Enzymol. **98:**241–260.
21. **Gruenberg, J.** 2001. The endocytic pathway: a mosaic of domains. Nat. Rev. Mol. Cell. Biol. **2:**721–730.
22. **Hansen, S. H., K. Sandvig, and B. van Deurs.** 1993. Clathrin and HA2 adaptors: effects of potassium depletion, hypertonic medium, and cytosol acidification. J. Cell Biol. **121:**61–72.
23. **Hassel, S., A. Eichner, M. Yakymovych, U. Hellman, P. Knaus, and S. Souchelnytskyi.** 2004. Proteins associated with type II bone morphogenetic protein receptor (BMPR-II) and identified by two-dimensional gel electrophoresis and mass spectrometry. Proteomics **4:**1346–1358.
24. **Hayes, S., A. Chawla, and S. Corvera.** 2002. TGF beta receptor internalization into EEA1-enriched early endosomes: role in signaling to Smad2. J. Cell Biol. **158:**1239–1249.
25. **Henis, Y. I., and O. Gutman.** 1983. Lateral diffusion and patch formation of H-2Kk antigens on mouse spleen lymphocytes. Biochim. Biophys. Acta **762:**281–288.
26. **Henley, J. R., E. W. Krueger, B. J. Oswald, and M. A. McNiven.** 1998. Dynamin-mediated internalization of caveolae. J. Cell Biol. **141:**85–99.
27. **Heuser, J.** 1989. Effects of cytoplasmic acidification on clathrin lattice morphology. J. Cell Biol. **108:**401–411.
28. **Hogan, B. L.** 1996. Bone morphogenetic proteins: multifunctional regulators of vertebrate development. Genes Dev. **10:**1580–1594.
29. **Hoodless, P. A., T. Haerry, S. Abdollah, M. Stapleton, M. B. O'Connor, L. Attisano, and J. L. Wrana.** 1996. MADR1, a MAD-related protein that functions in BMP2 signaling pathways. Cell **85:**489–500.
30. **Hooper, N. M.** 1999. Detergent-insoluble glycosphingolipid/cholesterol-rich membrane domains, lipid rafts and caveolae. Mol. Membr. Biol. **16:**145–156.
31. **Hua, X., J. Sakai, M. S. Brown, and J. L. Goldstein.** 1996. Regulated cleavage of sterol regulatory element binding proteins requires sequences on both sides of the endoplasmic reticulum membrane. J. Biol. Chem. **271:**10379–10384.
32. **Katzmann, D. J., M. Babst, and S. D. Emr.** 2001. Ubiquitin-dependent sorting into the multivesicular body pathway requires the function of a conserved endosomal protein sorting complex, ESCRT-I. Cell **106:**145–155.
33. **Klapisz, E., I. Sorokina, S. Lemeer, M. Pijnenburg, A. J. Verkleij, and P. M. van Bergen en Henegouwen.** 2002. A ubiquitin-interacting motif (UIM) is essential for Eps15 and Eps15R ubiquitination. J. Biol. Chem. **277:**30746–30753.
34. Reference deleted.
35. **Korchynskyi, O., and P. ten Dijke.** 2002. Identification and functional characterization of distinct critically important bone morphogenetic protein-specific response elements in the Id1 promoter. J. Biol. Chem. **277:**4883–4891.
36. **Kurzchalia, T. V., P. Dupree, R. G. Parton, R. Kellner, H. Virta, M. Lehnert, and K. Simons.** 1992. VIP21, a 21-kD membrane protein is an integral component of trans-Golgi-network-derived transport vesicles. J. Cell Biol. **118:**1003–1014.
37. **Lin, S., H. Y. Naim, A. C. Rodriguez, and M. G. Roth.** 1998. Mutations in the middle of the transmembrane domain reverse the polarity of transport of the influenza virus hemagglutinin in MDCK epithelial cells. J. Cell Biol. **142:**51–57.

38. **Liu, P., and R. G. Anderson.** 1999. Spatial organization of EGF receptor transmodulation by PDGF. Biochem. Biophys. Res. Commun. **261:**695–700.
39. **Lu, Z., J. T. Murray, W. Luo, H. Li, X. Wu, H. Xu, J. M. Backer, and Y. G. Chen.** 2002. Transforming growth factor beta activates Smad2 in the absence of receptor endocytosis. J. Biol. Chem. **277:**29363–29368.
40. **Massagué, J., and Y. G. Chen.** 2000. Controlling TGF-beta signaling. Genes Dev. **14:**627–644.
41. **McPherson, P. S., B. K. Kay, and N. K. Hussain.** 2001. Signaling on the endocytic pathway. Traffic **2:**375–384.
42. **Mitchell, H., A. Choudhury, R. E. Pagano, and E. B. Leof.** 2004. Ligand-dependent and -independent transforming growth factor-beta receptor recycling regulated by clathrin-mediated endocytosis and Rab11. Mol. Biol. Cell **15:**4166–4178.
43. **Munro, S.** 2003. Lipid rafts: elusive or illusive? Cell **115:**377–388.
44. **Niv, H., O. Gutman, Y. Kloog, and Y. I. Henis.** 2002. Activated K-Ras and H-Ras display different interactions with saturable nonraft sites at the surface of live cells. J. Cell Biol. **157:**865–872.
45. **Nohe, A., S. Hassel, M. Ehrlich, F. Neubauer, W. Sebald, Y. I. Henis, and P. Knaus.** 2002. The mode of bone morphogenetic protein (BMP) receptor oligomerization determines different BMP-2 signaling pathways. J. Biol. Chem. **277:**5330–5338.
46. **Nohe, A., E. Keating, T. M. Underhill, P. Knaus, and N. O. Petersen.** 2005. Dynamics and interaction of caveolin-1 isoforms with BMP-receptors. J. Cell Sci. **118:**643–650.
47. **Parton, R. G.** 2003. Caveolae—from ultrastructure to molecular mechanisms. Nat. Rev. Mol. Cell. Biol. **4:**162–167.
48. **Pelkmans, L., J. Kartenbeck, and A. Helenius.** 2001. Caveolar endocytosis of simian virus 40 reveals a new two-step vesicular-transport pathway to the ER. Nat. Cell Biol. **3:**473–483.
49. **Pelkmans, L., and M. Zerial.** 2005. Kinase-regulated quantal assemblies and kiss-and-run recycling of caveolae. Nature **436:**128–133.
50. **Penheiter, S. G., H. Mitchell, N. Garamszegi, M. Edens, J. J. Dore, Jr., and E. B. Leof.** 2002. Internalization-dependent and -independent requirements for transforming growth factor beta receptor signaling via the Smad pathway. Mol. Cell. Biol. **22:**4750–4759.
51. **Polo, S., S. Sigismund, M. Faretta, M. Guidi, M. R. Capua, G. Bossi, H. Chen, P. De Camilli, and P. P. Di Fiore.** 2002. A single motif responsible for ubiquitin recognition and monoubiquitination in endocytic proteins. Nature **416:**451–455.
52. **Poupon, V., S. Polo, M. Vecchi, G. Martin, A. Dautry-Varsat, N. Cerf-Bensussan, P. P. Di Fiore, and A. Benmerah.** 2002. Differential nucleocytoplasmic trafficking between the related endocytic proteins Eps15 and Eps15R. J. Biol. Chem. **277:**8941–8948.
53. **Puri, V., R. Watanabe, R. D. Singh, M. Dominguez, J. C. Brown, C. L. Wheatley, D. L. Marks, and R. E. Pagano.** 2001. Clathrin-dependent and -independent internalization of plasma membrane sphingolipids initiates two Golgi targeting pathways. J. Cell Biol. **154:**535–547.
54. **Rosenzweig, B. L., T. Imamura, T. Okadome, G. N. Cox, H. Yamashita, P. ten Dijke, C. H. Heldin, and K. Miyazono.** 1995. Cloning and characterization of a human type II receptor for bone morphogenetic proteins. Proc. Natl. Acad. Sci. USA **92:**7632–7636.
55. **Rothberg, K. G., J. E. Heuser, W. C. Donzell, Y. S. Ying, J. R. Glenney, and R. G. Anderson.** 1992. Caveolin, a protein component of caveolae membrane coats. Cell **68:**673–682.
56. **Runyan, C. E., H. W. Schnaper, and A. C. Poncelet.** 2005. The role of internalization in transforming growth factor beta1-induced Smad2 association with Smad anchor for receptor activation (SARA) and Smad2-dependent signaling in human mesangial cells. J. Biol. Chem. **280:**8300–8308.
57. **Sandvig, K., S. Olsnes, O. W. Petersen, and B. van Deurs.** 1987. Acidification of the cytosol inhibits endocytosis from coated pits. J. Cell Biol. **105:**679–689.
58. **Sargiacomo, M., M. Sudol, Z. Tang, and M. P. Lisanti.** 1993. Signal transducing molecules and glycosyl-phosphatidylinositol-linked proteins form a caveolin-rich insoluble complex in MDCK cells. J. Cell Biol. **122:**789–807.
59. **Sharma, D. K., J. C. Brown, A. Choudhury, T. E. Peterson, E. Holicky, D. L. Marks, R. Simari, R. G. Parton, and R. E. Pagano.** 2004. Selective stimulation of caveolar endocytosis by glycosphingolipids and cholesterol. Mol. Biol. Cell **15:**3114–3122.
60. **Sharma, P., S. Sabharanjak, and S. Mayor.** 2002. Endocytosis of lipid rafts: an identity crisis. Semin. Cell Dev. Biol. **13:**205–214.
61. **Sharma, P., R. Varma, R. C. Sarasij, Ira, K. Gousset, G. Krishnamoorthy, M. Rao, and S. Mayor.** 2004. Nanoscale organization of multiple GPI-anchored proteins in living cell membranes. Cell **116:**577–589.
62. **Shvartsman, D. E., M. Kotler, R. D. Tall, M. G. Roth, and Y. I. Henis.** 2003. Differently anchored influenza hemagglutinin mutants display distinct interaction dynamics with mutual rafts. J. Cell Biol. **163:**879–888.
63. **Simons, K., and E. Ikonen.** 1997. Functional rafts in cell membranes. Nature **387:**569–572.
64. **Simons, K., and D. Toomre.** 2000. Lipid rafts and signal transduction. Nat. Rev. Mol. Cell. Biol. **1:**31–39.
65. **Singh, R. D., V. Puri, J. T. Valiyaveettil, D. L. Marks, R. Bittman, and R. E. Pagano.** 2003. Selective caveolin-1-dependent endocytosis of glycosphingolipids. Mol. Biol. Cell **14:**3254–3265.
66. **Snyder, E. M., Y. Nong, C. G. Almeida, S. Paul, T. Moran, E. Y. Choi, A. C. Nairn, M. W. Salter, P. J. Lombroso, G. K. Gouras, and P. Greengard.** 2005. Regulation of NMDA receptor trafficking by amyloid-beta. Nat. Neurosci. **8:**1051–1058.
67. **Takei, K., P. S. McPherson, S. L. Schmid, and P. De Camilli.** 1995. Tubular membrane invaginations coated by dynamin rings are induced by GTP-gamma S in nerve terminals. Nature **374:**186–190.
68. **Thomsen, P., K. Roepstorff, M. Stahlhut, and B. van Deurs.** 2002. Caveolae are highly immobile plasma membrane microdomains, which are not involved in constitutive endocytic trafficking. Mol. Biol. Cell **13:**238–250.
69. **van der Bliek, A. M., T. E. Redelmeier, H. Damke, E. J. Tisdale, E. M. Meyerowitz, and S. L. Schmid.** 1993. Mutations in human dynamin block an intermediate stage in coated vesicle formation. J. Cell Biol. **122:**553–563.
70. **Wang, L. H., K. G. Rothberg, and R. G. Anderson.** 1993. Mis-assembly of clathrin lattices on endosomes reveals a regulatory switch for coated pit formation. J. Cell Biol. **123:**1107–1117.
71. **Warnock, D. E., and S. L. Schmid.** 1996. Dynamin GTPase, a force-generating molecular switch. Bioessays **18:**885–893.
72. **Yao, D., M. Ehrlich, Y. I. Henis, and E. B. Leof.** 2002. Transforming growth factor-beta receptors interact with AP2 by direct binding to beta2 subunit. Mol. Biol. Cell **13:**4001–4012.